

Received 7 July 2023, accepted 17 July 2023, date of publication 25 July 2023, date of current version 2 August 2023.

Digital Object Identifier 10.1109/ACCESS.2023.3298571

## RESEARCH ARTICLE

# Electromagnetic Modeling and Analysis of Multimaterial Cookware for Domestic Induction Heating

ALBERTO PASCUAL<sup>1</sup>, (Graduate Student Member, IEEE),  
JESÚS ACERO<sup>1</sup>, (Senior Member, IEEE), CLAUDIO CARRETERO<sup>2</sup>, (Senior Member, IEEE),  
SERGIO LLORENTE<sup>3</sup>, AND JOSÉ M. BURDIO<sup>1</sup>, (Senior Member, IEEE)

<sup>1</sup>Department of Electronic Engineering and Communications, University of Zaragoza, 50018 Zaragoza, Spain

<sup>2</sup>Department of Applied Physics, University of Zaragoza, 50009 Zaragoza, Spain

<sup>3</sup>Department of Research and Development, Bosch-Siemens Home Appliances Group, 50016 Zaragoza, Spain

Corresponding author: Alberto Pascual (a.pascual@unizar.es)

This work was supported in part by the Spanish MCIN/AEI/10.13039/501100011033 under Project PID2019-103939RB-I00, Project PDC2021-120898-I00, and Project CPP2021-008938; in part by EU through NextGenerationEU/PRTR and FEDER Programs; in part by the DGA-FSE; and in part by Bosch-Siemens Home Appliances Group.

**ABSTRACT** The performance of induction cooktops (inductor and electronic power converter) is closely related to the inductive properties of the cookware used. Traditionally, they are designed to work optimally with fully ferromagnetic cookware. However, multimaterial cookware with a bottom surface composed of a ferromagnetic material and small pieces of aluminum are nowadays more commonly used. Designing cooktops to also work optimally with this cookwares requires identifying the equivalent parameters,  $R_{eq}$  and  $L_{eq}$ , obtained from the electromagnetic models of the inductor-load system. Modeling multimaterial cookware, with a large number of inserts, complicates the model design and increases its computational cost. This work presents an equivalent model for multimaterial loads that allows the evaluation of the inductor performance and obtaining the equivalent parameters quickly and accurately. The multimaterial cookware is modeled as a disk of uniform material with equivalent electromagnetic properties,  $\mu_{r,eq}$  and  $\sigma_{eq}$ , which depend on the properties of each material and the proportion of area they occupy. The equivalent model has been validated by electromagnetic simulation using a FEA tool and by experimental results. Finally, based on the results obtained, an analysis has been carried out to evaluate the importance of design factors such as the choice of the cookware base material and the size, arrangement, and number of inserts.

**INDEX TERMS** Home appliances, induction heating, finite element simulation, magnetic devices.

## I. INTRODUCTION

High efficiency, automatic cookware detection, non-contact heat transfer, and speed of operation are some of the inherent features of domestic induction technology [1]. Its outstanding performance and other factors, such as the growing user concern about environmental aspects and safety, have led induction cooktops to displace conventional electric and gas heating technologies. Induction heating (IH), applied to the domestic scene, is a constantly evolving technology in

The associate editor coordinating the review of this manuscript and approving it for publication was Giambattista Gruosso<sup>1</sup>.

which research and development efforts in recent years have focused on its key enabling technologies: power electronic converters [2], [3], inductor system optimization [4], [5], magnetic materials [6], [7], deep learning techniques applied to IH [8], [9], control and modeling [10], [11], [12], [13], [14]. These advances have resulted in more secure and reliable operation, a better user experience, and faster applications.

An induction cooktop typically comprises the power electronics converter and the inductor-load system. As illustrated in Fig. 1, to facilitate the collaborative design of the converter and induction system, the inductor-load system is electrically modeled as an equivalent resistance  $R_{eq}$  connected in series

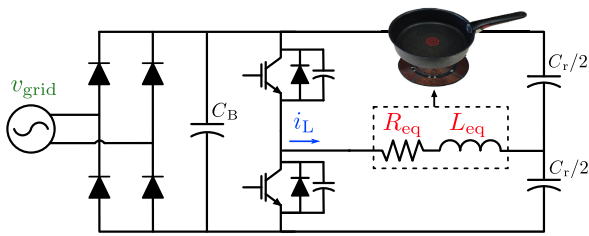


FIGURE 1. Simplified schematic of the induction cooktop.

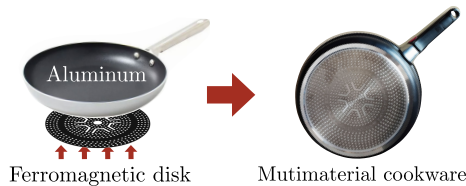


FIGURE 2. Composition of the multimaterial cookware.

to an equivalent inductance  $L_{eq}$ , where the  $R_{eq}$  represents the power dissipated, and  $L_{eq}$  represents the magnetic field of the system [15], [16]. The DC-AC converter supplies a variable frequency current, ranging from 20-100 kHz to the induction coil. This current produces an alternating magnetic field which, due to eddy current effects and, to a lesser extent, magnetic hysteresis losses, causes the load or cookware to heat up. The surface temperature profile of the cookware is determined by the positions of the turns in the inductor and the thermal properties of the materials [17].

One of the most commonly used materials in cookware for induction cooktops is stainless steel, which offers excellent efficiency results [18]. However, its low thermal conductivity (about 15 W/mK) leads to an uneven temperature distribution [17]. As a result, it complicates the cooking of temperature-sensitive dishes and impairs the cooking experience. Some proposals have been made to improve the heat distribution in cookware, ranging from unequally spaced turns of coils, for a more uniform temperature profile [19], [20], to movable inductors [21]. However, these solutions partially solve the problem, and further improvements are required.

Nowadays, cookware with a bottom surface composed of a ferromagnetic material and aluminum inserts is gaining importance in the market. This type of cookware usually consists of an aluminum cookware, to which a thin ferromagnetic disk with several holes is bonded at the bottom. The bonding process between the two elements depends on each manufacturer; however, the aluminum cookware is normally heated and bonded to the ferromagnetic disk by a stamping process, as schematically depicted in Fig. 2. Consequently, the bottom surface of the cookware is composed of ferromagnetic material whose initial slots have been filled by aluminum inserts. The excellent thermal conductivity of aluminum (237 W/mK) provide a better heat distribution over the cookware surface, solving the problem of the temperature

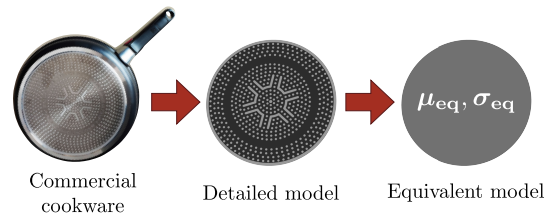


FIGURE 3. Modeling options for multimaterial cookware.

profile distribution to a large extent and, thus, providing a better cooking experience [22]. Aluminum is also light, durable, and affordable, reducing cookware weight and price. However, this thermal improvement results in worse electromagnetic behavior from the induction point of view, which is the origin of several problems. Some of these problems derive from current induction cooktops not being optimized for this type of cookware, with  $R_{eq}$  and  $L_{eq}$  parameters closer to aluminum than traditional cookware.

On the one hand, induction cooktops are equipped with a functionality that allows to auto-detect the presence of vessels on top of the coil [23]. The detection algorithm determines the presence of the cookware from the parameters  $R_{eq}$  and  $L_{eq}$  measured by the cooktop [8]. When the output of the algorithm falls within an accepted range of values, a command is sent to activate the coil. The range of accepted values is usually limited to the outputs that can be obtained with the  $R_{eq}$  and  $L_{eq}$  input parameters of ferromagnetic cookware. The inclusion of the aluminum inserts modifies these parameters, making detection more difficult and, in some cases leading to non-detection. Therefore, it is necessary to expand the number of cases with which the detection algorithm is trained to include the equivalent parameters of multimaterial cookware.

On the other hand, the performance of inductors and the cooktop converter is closely linked to the load's inductive properties and are traditionally designed to work optimally with ferromagnetic cookware. Modifying the optimal operating point of the cooktop for its use with multimaterial cookware requires selecting new components for the cooktop electronics tailored to their  $R_{eq}$  and  $L_{eq}$  parameters, i.e., select power devices (IGBT) with a nominal current that allow the nominal power to be supplied to different types of cookware or select new values for the resonant capacitors ( $C_r$ ) among others.

The calculation of the equivalent parameters ( $R_{eq}$  and  $L_{eq}$ ) and the inductors design are carried out by the electromagnetic modeling of the inductor-load system. In the literature, many papers deal with electromagnetic modeling in IH. Most of them are focused on industrial applications of induction heating with solenoidal coils [24], [25] or other applications based on eddy currents [26], [27], [28], [29]. Some specialized works in domestic IH that allow to obtain the  $R_{eq}$  and  $L_{eq}$  are [30], [31], and [32]. Focusing on cookware with aluminum inserts, a model analyzing its electrothermal behavior is presented in [22]. However, applying these

models to multimaterial cookware with a large number of inserts requires the implementation of a detailed model of their bottom surface, which complicates the model development and considerably increases the number of elements and its computational cost.

As shown in Fig. 3, this work presents a way to model the cookware with inserts as a disk of uniform material with equivalent electromagnetic properties,  $\mu_{r,eq}$  and  $\sigma_{eq}$ . This cookware model is considerably less complex to simulate and computationally much less demanding than a detailed model and allows the evaluation of the inductor performance and the obtaining of the equivalent circuit parameters quickly and accurately. This paper provides the expressions for determining the cookware equivalent relative magnetic permeability and equivalent electrical conductivity. At the same time, this model enables the classification of the large variety of multimaterial cookware available on the market, with different materials and inserts of different sizes and distributions, only by knowing their percentage of aluminum and diameter.

The model has been tested by electromagnetic simulation using a finite element program. The results obtained with a detailed model, composed of several materials and different sizes and quantities of inserts, have been compared with the corresponding results obtained with the equivalent model in each situation. In addition, it has been experimentally validated with commercial cookware and a configurable prototype in which the positions and materials of the different inserts can be varied. Finally, an analysis of the obtained results has been carried out, evaluating the importance of design factors such as the material of the base and the size, arrangement, and quantity of the inserts.

The paper is organized as follows. Section II provides the analytical expressions for estimating the equivalent material properties. Section III compares the equivalent model with the detailed one using finite element methods. The results obtained in the validation of the model have been used to analyze the influence on the cookware's performance of the ferromagnetic material used in the base and the size and quantity of the inserts. Section IV describes the experimental setup and shows the results. In Section V, some conclusions are drawn.

## II. ESTIMATION OF MATERIAL EQUIVALENT PROPERTIES

The inductor-load system usually consists of the cookware, the inductor, the ferrites, and the aluminum shielding. It can be electrically modeled using the equivalent circuit shown in Fig. 1. The circuit parameters,  $R_{eq}$  and  $L_{eq}$ , depend on several factors, which include the number of turns of the coil, the geometry and diameter of the coil, the arrangement and size of the ferrites, the geometry and electromagnetic properties of the cookware, and the operating frequency, among others [33].

The heat generation in IH is caused mainly by the dissipation of the induced currents in the cookware due to the Joule effect. Consequently, the influence on the equivalent circuit of the cookware electromagnetic properties, electrical

conductivity  $\sigma$  and relative magnetic permeability  $\mu_r$ , can be explained by means of the sheet resistance of the cookware materials at a given frequency ( $f$ ) [34]. This resistance can be deduced from the resistivity law,  $R = l/(w \cdot t \cdot \sigma)$ , and is usually expressed in Ohm per square. In this case, the length ( $l$ ) and width ( $w$ ) of the conductive area are considered to be equal, being only dependent on the thickness ( $t$ ), which in the context of induction heating corresponds to the skin depth ( $\delta$ ) [35]. The skin depth is the distance to the surface at which a sinusoidal electromagnetic field decays a 63%, thus determining the current conduction section. This distance is defined as:

$$\delta = \sqrt{1/(\pi f \mu_0 \mu_r \sigma)} \quad (1)$$

being  $\mu_0$  the magnetic permeability of vacuum. Therefore, the sheet resistance per square can be expressed as follows:

$$R_{sheet} = \frac{1}{\delta \sigma} = \sqrt{\frac{\pi f \mu_0 \mu_r}{\sigma}} \quad (2)$$

A qualitative assessment of the inductor-load system performance can be made using (2). In cases where this resistance is too high, as in the case of non-conductive materials (several k $\Omega$  per square), it cannot be induced sufficient current to achieve perceptible heating by the Joule effect. On the other hand, in cases where  $R_{sheet}$  is too low, as in the case of materials that are good conductors but not ferromagnetic (copper, aluminum), the power dissipation achieved by the Joule effect is also low [32].

The bottom surface of the cookware with inserts is usually comprised of a main part made of ferromagnetic material and small pieces of a material with high thermal conductivity, usually aluminum. The ratio of the area occupied by the inserts ( $A_{ins}$ ) to the total surface area of the cookware ( $A_{tot}$ ) can be expressed as  $\chi_{ins}$ :

$$\chi_{ins} = \frac{A_{ins}}{A_{tot}} \quad (3)$$

and therefore, the area occupied by the ferromagnetic material is  $(1-\chi_{ins})$ . The distribution of the magnetic field produced by the inductor tries to follow the guide provided by the ferromagnetic part of the cookware, so in the first instance, it could be considered that the cookware performance is uniquely proportional to the area occupied by the ferromagnetic material and its sheet resistance. However, although aluminum is not ferromagnetic, it is a good electrical conductor through which currents can be induced, and eddy currents can flow. Therefore, the inductive performance of the cookware is also affected by the percentage of aluminum on the bottom surface. Thus, the total power dissipated by the joule effect can be considered proportional to the sheet resistance of each material and the proportional area they occupy. These considerations suggest that multimaterial cookware, at least in a first approximation, could be replaced by a single-material cookware with equivalent sheet resistance, in which the influence of each of the materials is proportional to the area they occupy

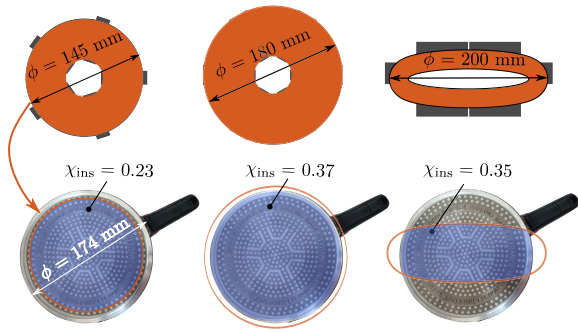


**FIGURE 4.** Different inductor geometries, above. Below, marked in blue, are the intersection zones between the cookware and the inductors used for the  $\chi_{ins}$  calculation.

in relation to the total area of the cookware that is affected by the magnetic field.

The sheet resistance of the equivalent cookware depends on the electromagnetic properties of both, the inserts and the ferromagnetic material; in other words,  $\sigma_{eq}$  and  $\mu_{r,eq}$  contain the cross products of the properties of both materials. This way does not allow the visualization of the influence of each material on the equivalent properties. Therefore, it is proposed to deal with the equivalent properties separately. This proposal will be validated by means of simulation and experimental results, and is implemented as follows. In (2), it can be observed that the Joule power losses in the cookware are widely affected by the value of the square root of its relative magnetic permeability ( $R_{sheet} \propto \sqrt{\mu_r}$ ) and the inverse of the square root of its electrical conductivity ( $R_{sheet} \propto \sqrt{\sigma}^{-1}$ ). Therefore, it could be considered that the square root of the equivalent magnetic permeability can be expressed as the sum of the square roots of each of the materials' permeabilities multiplied by the proportional area they occupy with respect to the total area:

$$\mu_{r,eq} = \left( (1 - \chi_{ins})\sqrt{\mu_{r,fe}} + \chi_{ins}\sqrt{\mu_{r,ins}} \right)^2 \quad (4)$$

similarly, the equivalent electrical conductivity, which has a dependence proportional to the inverse of the square root of each of the  $\sigma$  of its constituent materials, can be expressed as follows:

$$\sigma_{eq} = \left( \frac{1}{\frac{1 - \chi_{ins}}{\sqrt{\sigma_{fe}}} + \frac{\chi_{ins}}{\sqrt{\sigma_{ins}}}} \right)^2 \quad (5)$$

where  $\mu_{r,eq}$  and  $\sigma_{eq}$  are the equivalent properties of the cookware, and the subscripts *fe* and *ins* correspond to the ferromagnetic part of the cookware base and the aluminum inserts respectively. This assumption is valid for the area affected by the magnetic field and in which currents are induced. Thus, although the equivalent disk introduced in the model has the same dimensions as the original cookware, the percentage of aluminum ( $\chi_{ins}$ ) is only weighted by the area in which the magnetic field is incident on the cookware.

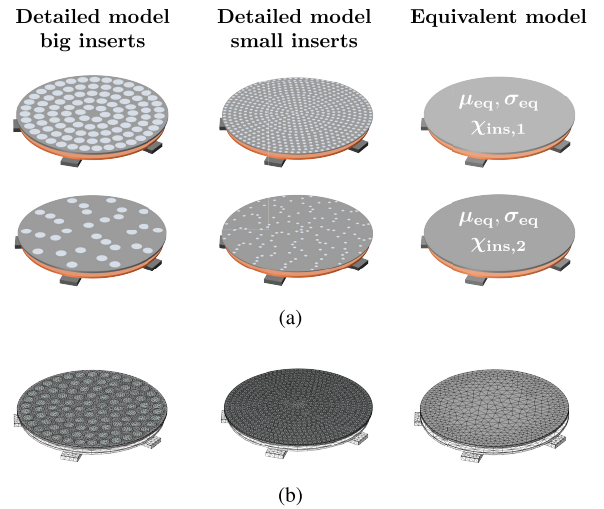


**FIGURE 5.** Models used to analyze the influence of insert size on the multimaterial cookware (a) and mesh employed in each one (b).

The inductors used in domestic IH are designed to transmit power to the entire surface of the cookware and the distance between the inductor and the load is small, so it can be assumed that the magnetic field incident on the load has the same dimensions and geometry as the inductor. So, the  $\chi_{ins}$  value can be calculated in the area where the cookware and the inductor intersect. This condition is illustrated in Fig. 4, where the intersection area (marked in blue) between a commercial cookware and several inductors typically used in commercial cooktops is depicted. Thus, in spite of using the same cookware, for the study of each inductor, different values of  $\chi_{ins}$  are introduced in the calculation of the (4) and the (5). In the case of the 145 mm inductor, the inserts occupy 23% of the total area in which the magnetic field is incident ( $\chi_{ins} = 0.23$ ). Whereas, in the case of the 180 mm diameter inductor and the elliptical inductor, as they cover the area of the outer ring, which is made only by aluminum, the percentage of aluminum in relation to the total area covered increases considerably, up to  $\chi_{ins}$  of 0,37 and 0,35 respectively.

### III. MODEL VALIDATION AND DESIGN ANALYSIS

Given the wide variety of cookware on the market, it is convenient to check that the model is valid for any ferromagnetic material used in the base and any size, quantity, and arrangement of the inserts. For this purpose, a finite element model has been developed using the commercial FEA tool COMSOL Multiphysics, which allows the simulation of the electromagnetic phenomena in the induction heating system. The analyzed IH system consists of a cookware placed above a planar coil and an aluminum plate set under the rest of the elements to shield the electronic components under the induction system. It also incorporates ferrite bars between the coil and the shielding to increase the coupling with the cookware. The FEA model is based on those developed by [33] and [36], which allow to obtain the  $R_{eq}$  and  $L_{eq}$  parameters of the equivalent circuit of the inductor-load system.



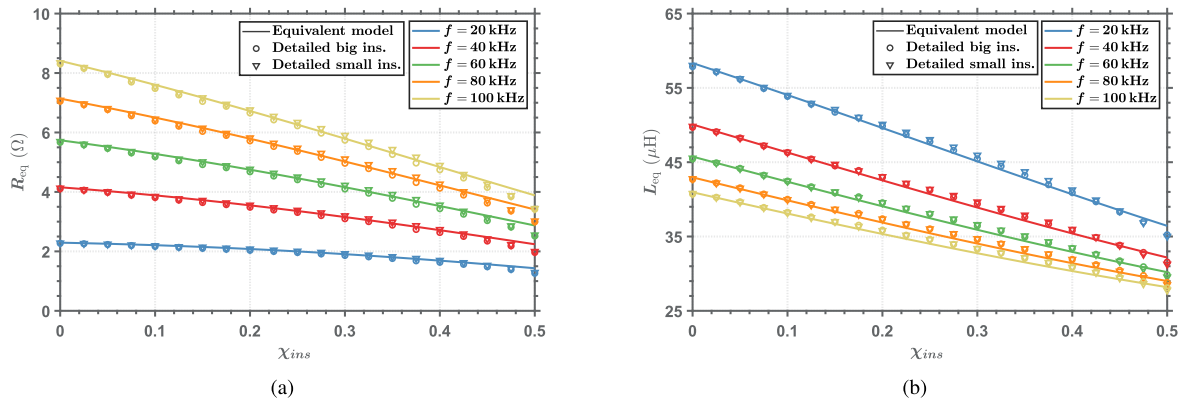


**FIGURE 6.** Equivalent circuit parameters,  $R_{eq}$ (a) and  $L_{eq}$ (b), depending on the percentage of aluminum in the base of the cookware and the model used for its calculation.

### A. INSERT SIZE INFLUENCE

Three different models have been used to analyze the performance of the equivalent model as a function of insert size in multimaterial cookware. The simulation models consider the same planar inductor of 24 turns and 145 mm diameter, whose diameter coincides with that of the cookware. The percentage of material occupied by the inserts is the same in the three simulations. The main material of the cookware base is stainless steel with electrical conductivity  $\sigma_{fe} = 1,1 \cdot 10^6$  S/m and a relative magnetic permeability  $\mu_{r,fe} = 100$ . The material of the inserts is aluminum ( $\mu_{r,ins} = 1$  and  $\sigma_{ins} = 2,2 \cdot 10^7$  S/m). As shown in Fig. 5(a), the first model is a detailed model of the cookware base with big inserts, where each insert occupies 0.5% of the bottom surface area. The second is also a detailed model with small inserts, where each insert only takes 0.07143% of the total area. As seen in Fig. 5(b), the smaller the inserts, the more elements will be needed in the mesh. In these two models, the number of inserts has been varied to modify the percentage of aluminum in the base from 0 to 50%. The last model is a cookware made of a single material whose properties are calculated with the equations (4) and (5) and whose values vary according to the percentage of aluminum  $\chi_{ins}$ .

Fig. 6 shows the equivalent resistance and inductance values obtained for the considered cases. As seen in the simulations, the equivalent circuit parameters of the inductor-load system are very similar. As expected, the electrical performance of the cookware is largely influenced by the percentage of aluminum in it. However, the size of the insert has a minimal influence on its electrical performance, so it is possible to choose the dimensions that are of most interest to improve the thermal distribution of the cookware.

It is also worth noting the differences between the computational cost required by the models for each case with different frequencies and percentages of aluminum. The computer used to carry out the simulations has a 2.90 GHz i9-8950HK processor and 32 GB of RAM. The simulation time required in each case of  $f$  and  $\chi_{ins}$  was 15.3 seconds in

the equivalent model. In contrast, due to the more significant number of elements required by the mesh in the other models, it took 1 min and 18.9 seconds on average in the model with big inserts and 8 min and 3.8 seconds in the model with small inserts. Thus, the equivalent model saves considerable computational time and requires less effort to prepare and develop.

### B. MATERIALS ANALYSIS

Another fundamental aspect on the cookware with inserts design is the choice of materials for the base. As mentioned above, the inserts must have good thermal conductivity and be cost-effective, so the ideal material for them is aluminum. However, when it comes to choosing the ferromagnetic part of the cookware base, there are more options, and it requires a more exhaustive analysis of the optimal selection of material.

In Fig. 7, the influence of the electromagnetic properties of the equivalent disk on the electrical performance and efficiency of the inductor-load system is shown. It has been analyzed in the same system as the previous section at an operating frequency of 30 kHz. Considering that the inductor is wound with 24 turns of a 32-strand Litz wire of 0.3 mm diameter, the efficiency has been estimated from the method proposed by [18] and [37]. The dependence of the equivalent resistance on the electromagnetic properties of the cookware is shown in Fig. 7(a). It can be seen that there is an optimal relationship between  $\sigma_{eq}$  and  $\mu_{r,eq}$ , where the  $R_{eq}$  and hence the power dissipated in the cookware is maximum. Fig. 7(b) shows that the system becomes more inductive as the relative magnetic permeability increases. Lastly, in Fig. 7(c), it can be observed that the efficiency also has an optimum operating point, very similar to that of the equivalent resistance. Considering these two parameters, it can be said that for a  $\sigma_{eq}/\mu_{r,eq}$  ratio between  $5 \cdot 10^3$  and  $2 \cdot 10^4$  for the cookware equivalent material, optimum results in terms of delivered power and efficiency can be obtained. When this ratio is exceeded, the sheet resistance of the material is too high, and it cannot be

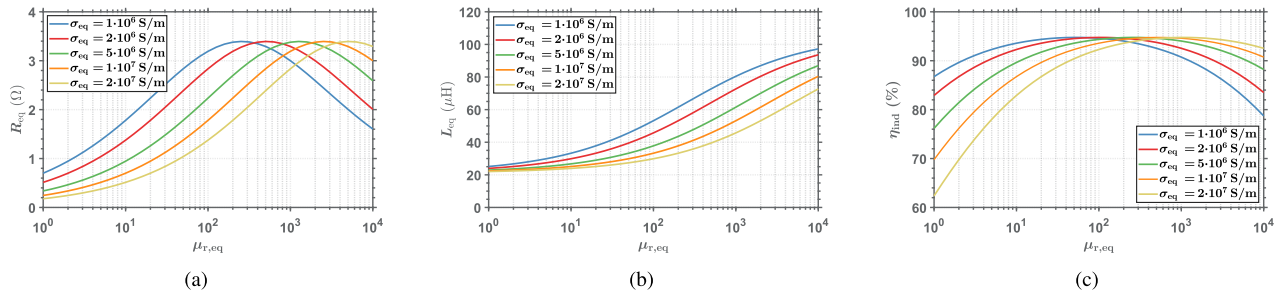


**FIGURE 7.** Influence of the  $\mu_r$  and  $\sigma$  of the equivalent disk material on the equivalent resistance (a), equivalent inductance (b), and efficiency (c) of the inductor-load system at a working frequency of 30 kHz.

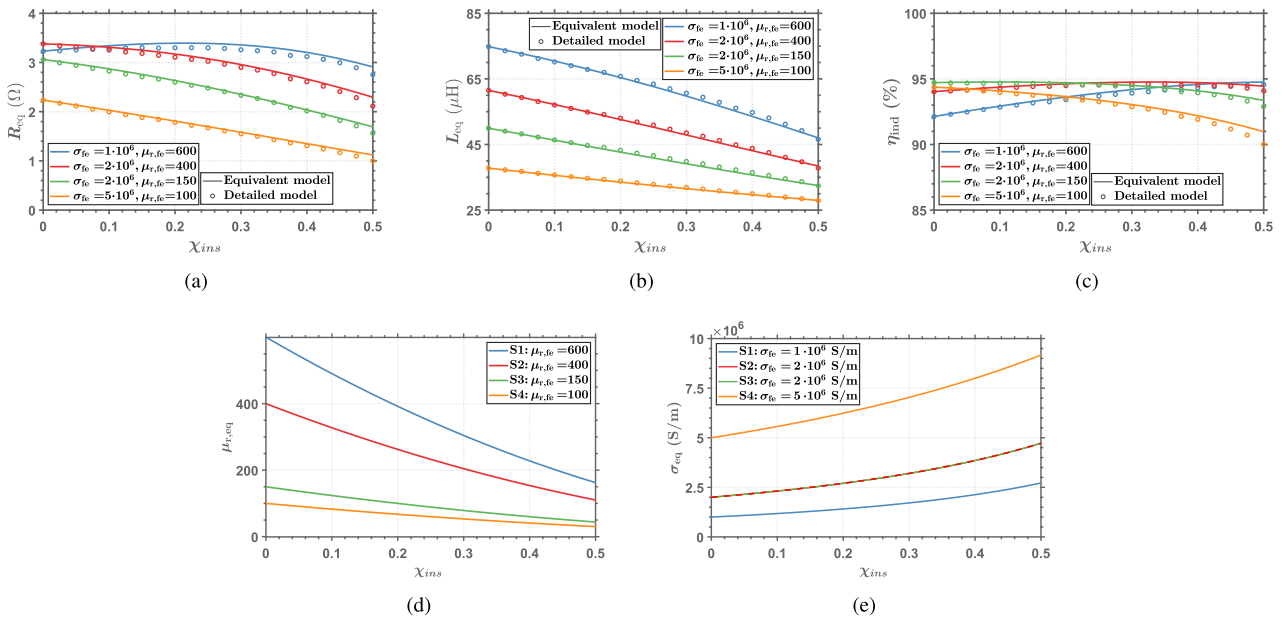


**FIGURE 8.** Variation of  $R_{eq}$ (a),  $L_{eq}$ (b), inductor-load efficiency(c), equivalent relative magnetic permeability (d) and equivalent electrical conductivity (e) with respect to the percentage of aluminum in the bottom of the cookware, whose base is composed of different steel alloys at an operating frequency of 30 kHz.

induced sufficiently current to achieve perceptible heating by the Joule effect. In the case where the material's sheet resistance is too low, the  $R_{eq}$ , and hence the power dissipation achieved by the Joule effect, are also low.

Fig. 8 shows how the cookware behaves with four different base materials with respect to the percentage of aluminum inserts they contain. The materials used correspond to four steel alloys, represented by different  $\mu_{r,fe}$  and  $\sigma_{fe}$ . Two simulations are compared, one with the equivalent disk and the other with the detailed model. Fig. 8(a) shows the variation of the equivalent resistance with respect to the  $\chi_{ins}$  in several steel alloys. From it, it can be extracted that, in general, introducing a higher percentage of inserts acts to the detriment of the electrical performance of the cookware. However, including aluminum inserts allow some alloys to reach an optimum ratio of equivalent  $\sigma_{eq}/\mu_{r,eq}$  and increase the dissipated power. From Fig. 8(b), it can be observed that within the range of values in the electromagnetic

properties of the steel alloys ( $\mu_{r,fe}$  from 100-1000 and  $\sigma_{fe}$  from  $1 \cdot 10^6$ - $1 \cdot 10^7$  S/m), the inclusion of inserts will always result in a lower equivalent inductance, since the increase in the proportion of non-ferromagnetic material causes the  $\mu_{r,eq}$  to decrease. Fig. 8(c) shows the inductor-load efficiency. As with the  $R_{eq}$ , the importance of using a quality alloy for the cookware's bottom surface, such as those marked by the blue and red lines, can be extracted. Although these steel alloys may be more expensive than others, it may allow adding a more significant amount of inserts, with their respective thermal improvement, reducing the amount of steel required in the base and satisfying the requirements of good equivalent resistance and efficiency. Fig. 8(d) and Fig. 8(e) show the variation of the equivalent electromagnetic properties of the cookware as a function of the percentage of inserts contained in each of the alloys.

Finally, it can be extracted from the results obtained from these simulations that the equivalent disk model also gives



**FIGURE 9.** The bottom surface of the commercial cookware with small inserts (a) and the cookware prototype with detachable inserts (b).

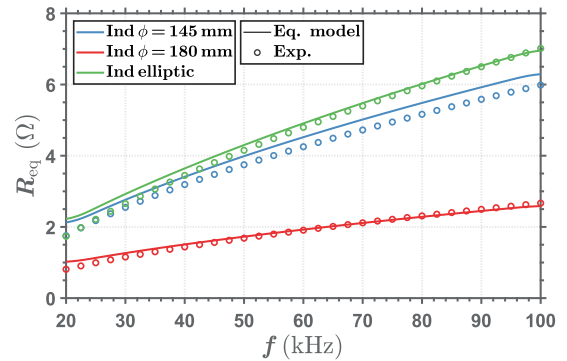
good results for different types of ferromagnetic materials with any amount, up to 50%, of aluminum inserts in the cookware base.

#### IV. EXPERIMENTAL VERIFICATION

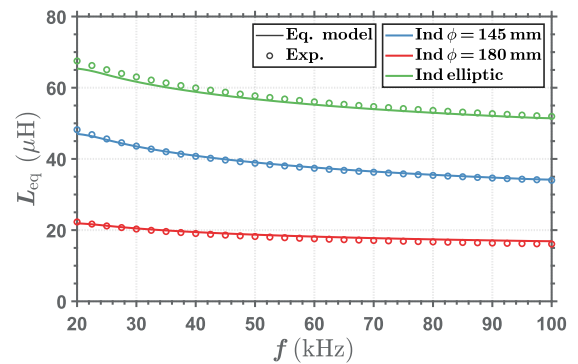
The verification of the model has been carried out by comparing the parameters of the equivalent circuit of the inductor-load system obtained experimentally and those obtained by the simulation of the equivalent cookware model. The frequency-dependent equivalent resistance,  $R_{eq}$ , and inductance,  $L_{eq}$ , of the system, were measured using a precision LCR meter (Agilent E4980A). The LCR was connected to the inductor terminals and measured the series resistance and inductance of the complete system (inductor, load, ferrites and aluminum shielding). The experimental measurements correspond to small-signal conditions; therefore, there are no thermal effects or variations of electromagnetic properties due to changes in the excitation level. The frequency range studied is between 20-100 kHz, corresponding to the interest range for domestic induction heating.

Two different tests have been carried out to verify the proposal of this work. The first aims to probe whether the model can electrically characterize commercial cookware with inserts in any inductor. For this purpose, the cookware shown in Fig. 9(a) has been used in the inductors shown in Fig. 4. The cookware is composed of a steel alloy with a  $\sigma_{fe}$  of  $1.1 \cdot 10^6$  S/m and a  $\mu_{r,fe}$  of 100 and aluminum inserts ( $\sigma_{ins} = 2.2 \cdot 10^7$  S/m,  $\mu_{r,ins} = 1$ ). The cookware has been modeled by means of a disk with the same diameter as the base of the commercial cookware under analysis ( $\phi = 174$  mm) and a variable  $\chi_{ins}$ , depending on the inductor. As mentioned above, as each of the inductors intersects differently with the cookware (Fig. 4), a different  $\chi_{ins}$  has been used in (4) and (5) for the calculation of the equivalent electromagnetic properties.  $\chi_{ins} = 0,23$  in the inductor with  $\phi = 145$  mm and 24 turns,  $\chi_{ins} = 0,37$  in the inductor with  $\phi = 180$  mm and 19 turns and  $\chi_{ins} = 0,35$  in the elliptic inductor with 22 turns. In Fig. 10, the comparison between  $R_{eq}$ (a) and  $L_{eq}$ (b) measured and calculated with the equivalent model is shown. It can be observed that the results obtained experimentally with the different inductors agree with those obtained with the equivalent model.

The other experiment has been carried out with the prototype shown in Fig. 9(b) on an inductor of 17 turns and



(a)



(b)

**FIGURE 10.** Comparison between simulated results with the equivalent model and experimental results for commercial cookware in various inductors. (a) Equivalent resistance. (b) Equivalent inductance.

210 mm diameter. This prototype has a diameter of 230 mm. It is composed of a steel alloy with a  $\sigma_{fe}$  of  $2 \cdot 10^6$  S/m and a  $\mu_{r,fe}$  of 225 in the base (area painted in black) and two types of detachable inserts, one of the same material as the base and the other made of aluminum. Consequently, the percentage of aluminum inserts can be varied. In this experiment, several measurements have been performed using the same amount of aluminum inserts but distributed in different ways along the cookware's surface, validating that the model is a good approximation regardless of the distribution of the inserts. The results of this experiment are shown in Fig. 11. In it, 22 inserts of aluminum, marked in red, and the rest of the same material as the base have been distributed in four ways (Fig. 11(c)). Each insert has a diameter of 8 mm, so the twenty-two inserts correspond to a  $\chi_{ins}$  of 0.1276. As can be seen from the experimental results, the variation in the position of the aluminum inserts has hardly affected the equivalent resistance and inductance. Like in the previous experiment, the agreement between the model and the measurements is satisfactory.

It should be noted that both experiments have been carried out with cookware with different insert sizes, different percentages of aluminum and different materials, as well as tested with different inductors, increasing the situations for the model validation.

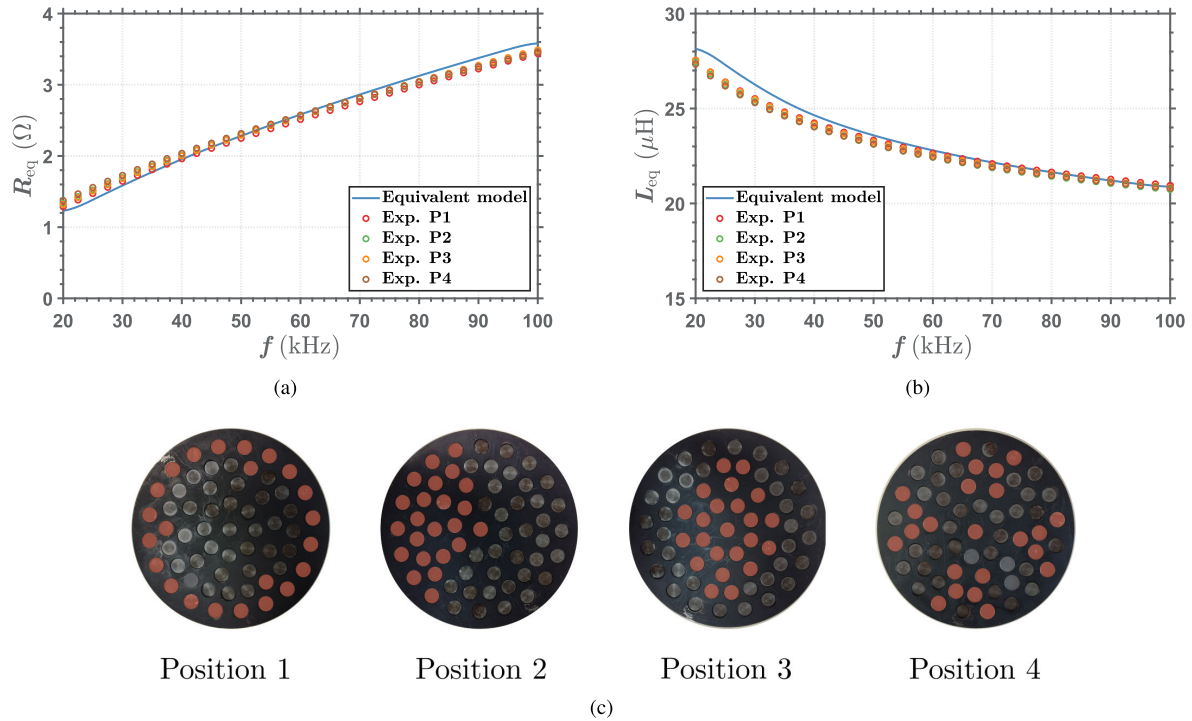


**FIGURE 11.** Comparison between simulated results with the equivalent model and the experimental measures for different distributions of inserts along the cookware surface.  $R_{eq}$  (a),  $L_{eq}$  (b), and distribution of inserts in each measurement (c).

**V. CONCLUSION**

This work presents an electromagnetic equivalent model for multimaterial loads in IH. It is proposed to model them as a homogeneous material with equivalent electromagnetic properties. Compared to a detailed model, the proposed model requires much less computational time and does not require the exact replication of the geometry, which usually consists of a large number of small inserts. The modeling using equivalent electromagnetic properties allows the simulation of multimaterial cookware using 2D axisymmetric and analytical models, further simplifying the model since the 3D simulations can be computationally intensive. This cookware characterization method simplifies the mapping of equivalent parameters of existing cookware on the market to classify them for identification and detection purposes. In addition, it facilitates the design of inductors and power converters for induction cooktops optimized for multimaterial loads.

From the results obtained, it can be extracted that, for a constant percentage of aluminum, the size of the inserts does not significantly influence the electromagnetic performance of the system, allowing to choose the most beneficial insert size to improve the heat transfer. As for the choice of materials, the best option for the ferromagnetic part of the cookware is to choose a material with high magnetic permeability and low conductivity so that when combined with the aluminum inserts, they can achieve optimum equivalent electromagnetic properties with a  $\sigma_{eq}/\mu_{r,eq}$  ratio between  $5 \cdot 10^3$  and  $2 \cdot 10^4$ .

The experimental measurements verified that the equivalent model obtains good results from 12% to 37% of aluminum in the cookware base, with various types of inductors and inserts with different arrangements and sizes. Furthermore, through the FEA simulation, with the detailed and equivalent model, it has been proven that satisfactory results are achieved over the whole range from 0% to 50% of aluminum in the cookware’s base.

**REFERENCES**

- [1] J. Acero, J. Burdío, L. Barragán, D. Navarro, R. Alonso, J. García, F. Monterde, P. Hernández, and S. L. I. Garde, “Domestic induction appliances,” *IEEE Ind. Appl. Mag.*, vol. 16, no. 2, pp. 39–47, Mar. 2010.
- [2] R. C. M. Gomes, M. A. Vitorino, D. A. Acevedo-Bueno, and M. B. D. R. Corrêa, “Multiphase resonant inverter with coupled coils for AC–AC induction heating application,” *IEEE Trans. Ind. Appl.*, vol. 56, no. 1, pp. 551–560, Jan. 2020.
- [3] S. Komeda and H. Fujita, “A phase-shift-controlled direct AC-to-AC converter for induction heaters,” *IEEE Trans. Power Electron.*, vol. 33, no. 5, pp. 4115–4124, May 2018.
- [4] H. Bensaidane, T. Lubin, S. Mezani, Y. Ouazir, and A. Rezzoug, “A new topology for induction heating system with PM excitation: Electromagnetic model and experimental validations,” *IEEE Trans. Magn.*, vol. 51, no. 10, pp. 1–11, Oct. 2015.
- [5] E. Jang, M. J. Kwon, S. M. Park, H. M. Ahn, and B. K. Lee, “Analysis and design of flexible-surface induction-heating cooktop with GaN–HEMT-based multiple inverter system,” *IEEE Trans. Power Electron.*, vol. 37, no. 10, pp. 12865–12876, Oct. 2022.
- [6] A. Pascual, J. Acero, C. Carretero, and S. Llorente, “Experimental characterization of materials with controlled Curie temperature for domestic induction heating applications,” in *Proc. IECON Ind. Electron. Conf.*, Oct. 2021, pp. 1–6.



- [7] A. Pascual, J. Acero, S. Llorente, C. Carretero, and J. M. Burdio, "Self-adaptive overtemperature protection materials for safety-centric domestic induction heating applications," *IEEE Access*, vol. 11, pp. 1193–1201, 2023.
- [8] J. Villa, D. Navarro, A. Dominguez, J. I. Artigas, and L. A. Barragan, "Vessel recognition in induction heating appliances—A deep-learning approach," *IEEE Access*, vol. 9, pp. 16053–16061, 2021.
- [9] O. Lucia, D. Navarro, P. Guillén, H. Sarnago, and S. Lucia, "Deep learning-based magnetic coupling detection for advanced induction heating appliances," *IEEE Access*, vol. 7, pp. 181668–181677, 2019.
- [10] L. Codecasa, P. Alotto, and F. Moro, "Fast solution of induction heating problems by structure-preserving nonlinear model order reduction," *IEEE Trans. Magn.*, vol. 52, no. 3, pp. 1–4, Mar. 2016.
- [11] K. Roppert, F. Toth, and M. Kaltenbacher, "Modeling nonlinear steady-state induction heating processes," *IEEE Trans. Magn.*, vol. 56, no. 3, pp. 1–4, Mar. 2020.
- [12] A. Pascual, J. Acero, J. M. Burdio, C. Carretero, and S. Llorente, "Electrothermal analysis of temperature-limited loads for domestic induction heating applications," in *Proc. IECON Ind. Electron. Conf.*, Oct. 2022, pp. 1–6.
- [13] S. Yin, X. Ma, C. Luo, J. Wang, and X. Zhu, "Modeling and analysis of transient performance for induction heating system considering frequency-dependent inductive load," *IEEE Trans. Magn.*, vol. 55, no. 6, pp. 1–4, Jun. 2019.
- [14] R. Torchio, L. Codecasa, L. Di Rienzo, and F. Moro, "Fast uncertainty quantification in low frequency electromagnetic problems by an integral equation method based on hierarchical matrix compression," *IEEE Access*, vol. 7, pp. 163919–163932, 2019.
- [15] F. Forest, E. Laboure, F. Costa, and J. Y. Gaspard, "Principle of a multi-load/single converter system for low power induction heating," *IEEE Trans. Power Electron.*, vol. 15, no. 2, pp. 223–230, Mar. 2000.
- [16] H. W. Koertzen, J. D. van Wyk, and J. A. Ferreira, "Design of the half-bridge, series resonant converter for induction cooking," in *Proc. Power Electron. Spec. Conf.*, Jun. 1995, pp. 729–735.
- [17] I. Cabeza-Gil, B. Calvo, J. Grasa, C. Franco, S. Llorente, and M. A. Martínez, "Thermal analysis of a cooking pan with a power control induction system," *Appl. Thermal Eng.*, vol. 180, Nov. 2020, Art. no. 115789.
- [18] J. Acero, C. Carretero, R. Alonso, and J. M. Burdio, "Quantitative evaluation of induction efficiency in domestic induction heating applications," *IEEE Trans. Magn.*, vol. 49, no. 4, pp. 1382–1389, Apr. 2013.
- [19] S.-Y. Hahn, H.-S. Roh, K. Choi, and J.-K. Byun, "Optimal design procedure for a practical induction heating cooker," *IEEE Trans. Magn.*, vol. 36, no. 4, pp. 1390–1393, Jul. 2000.
- [20] M. Aoyama, W. Thimm, M. Knoch, and L. Ose, "Proposal and challenge of Halbach array type induction coil for cooktop applications," *IEEE Open J. Ind. Appl.*, vol. 2, pp. 168–177, 2021.
- [21] F. Sanz, C. Sagues, and S. Llorente, "Induction heating appliance with a mobile double-coil inductor," *IEEE Trans. Ind. Appl.*, vol. 51, no. 3, pp. 1945–1952, May 2015.
- [22] E. Plumed, I. Lope, and J. Acero, "Modeling and design of cookware for induction heating technology with balanced electromagnetic and thermal characteristics," *IEEE Access*, vol. 10, pp. 83793–83801, 2022.
- [23] A. Bono-Nuez, B. Martin-del-Brio, C. Bernal-Ruiz, F. J. Perez-Cebolla, A. Martinez-Iturbe, and I. Sanz-Gorrrachategui, "The inductor as a smart sensor for material identification in domestic induction cooking," *IEEE Sensors J.*, vol. 18, no. 6, pp. 2462–2470, Mar. 2018.
- [24] U. Lütke and D. Schulze, "Numerical simulation of continuous induction steel bar end heating with material properties depending on temperature and magnetic field," *IEEE Trans. Magn.*, vol. 34, no. 5, pp. 3106–3109, Sep. 1998.
- [25] F. Dughiero, M. Forzan, C. Pozza, and E. Sieni, "A translational coupled electromagnetic and thermal innovative model for induction welding of tubes," *IEEE Trans. Magn.*, vol. 48, no. 2, pp. 483–486, Feb. 2012.
- [26] D. Zheng and X. Guo, "Analytical prediction and analysis of electromagnetic-thermal fields in PM eddy current couplings with injected harmonics into magnet shape for torque improvement," *IEEE Access*, vol. 8, pp. 60052–60061, 2020.
- [27] X. Yang, Y. Liu, and L. Wang, "An improved analytical model of permanent magnet eddy current magnetic coupler based on electromagnetic-thermal coupling," *IEEE Access*, vol. 8, pp. 95235–95250, 2020.
- [28] S. Hansson and M. Fisk, "Simulations and measurements of combined induction heating and extrusion processes," *Finite Elements Anal. Des.*, vol. 46, no. 10, pp. 905–915, Oct. 2010.
- [29] D. Hömberg, Q. Liu, J. Montalvo-Urquiza, D. Nadolski, T. Petzold, A. Schmidt, and A. Schulz, "Simulation of multi-frequency-induction-hardening including phase transitions and mechanical effects," *Finite Elements Anal. Des.*, vol. 121, pp. 86–100, Nov. 2016.
- [30] M.-S. Huang, C.-C. Liao, Z.-F. Li, Z.-R. Shih, and H.-W. Hsueh, "Quantitative design and implementation of an induction cooker for a copper pan," *IEEE Access*, vol. 9, pp. 5105–5118, 2021.
- [31] Z. Li, Q. Chen, S. Zhang, X. Ren, and Z. Zhang, "A novel domestic SE-IH with high induction efficiency and compatibility of nonferromagnetic vessels," *IEEE Trans. Ind. Electron.*, vol. 68, no. 9, pp. 8006–8016, Sep. 2021.
- [32] W. Han, K. T. Chau, C. Jiang, and W. Liu, "All-metal domestic induction heating using single-frequency double-layer coils," *IEEE Trans. Magn.*, vol. 54, no. 11, pp. 1–5, Nov. 2018.
- [33] J. Acero, R. Alonso, J. M. Burdio, L. A. Barragan, and D. Puyal, "Analytical equivalent impedance for a planar circular induction heating system," *IEEE Trans. Magn.*, vol. 42, no. 1, pp. 84–86, Jan. 2006.
- [34] T. Tanaka, "A new induction cooking range for heating any kind of metal vessels," *IEEE Trans. Consum. Electron.*, vol. 35, no. 3, pp. 635–641, Aug. 1989.
- [35] A. Canova, F. Dughiero, F. Fasolo, M. Forzan, F. Freschi, L. Giaccone, and M. Repetto, "Identification of equivalent material properties for 3-D numerical modeling of induction heating of ferromagnetic workpieces," *IEEE Trans. Magn.*, vol. 45, no. 3, pp. 1851–1854, Mar. 2009.
- [36] J. Acero, C. Carretero, I. Millán, Ó. Lucía, R. Alonso, and J. M. Burdio, "Analysis and modeling of planar concentric windings forming adaptable-diameter burners for induction heating appliances," *IEEE Trans. Power Electron.*, vol. 26, no. 5, pp. 1546–1558, May 2011.
- [37] A. Pascual, J. Acero, S. Llorente, C. Carretero, and J. M. Burdio, "Small-sized immersible water heaters for domestic induction heating technology," *IEEE Access*, vol. 11, pp. 51480–51489, 2023.



**ALBERTO PASCUAL** (Graduate Student Member, IEEE) received the M.Sc. degree in electronic systems engineering from the Polytechnic University of Madrid, Spain, in 2016, and the degree in industrial technologies engineering from the University of Zaragoza, where he is currently pursuing the Ph.D. degree. He is a member of Instituto de Investigación en Ingeniería de Aragón (I3A), Power Electronics and Microelectronics Group (GEPM). His main research interests include the analysis and development of advanced technologies for induction heating focused on self-protection.



**JESÚS ACERO** (Senior Member, IEEE) received the M.Sc. and Ph.D. degrees in electrical engineering from the University of Zaragoza, Zaragoza, Spain, in 1992 and 2005, respectively. From 1992 to 2000, he worked on several industry projects, especially focused on custom power supplies for research laboratories. Since 2000, he has been with the Department of Electronic Engineering and Communications, University of Zaragoza, where he is currently a Professor. His main research interests include resonant converters for induction heating applications, inductive-type load modeling, and electromagnetic modeling. He is a member of the IEEE Power Electronics Society, the IEEE Industrial Electronics Society, and the IEEE Magnetics Society. He is also a member of Instituto de Investigación en Ingeniería de Aragón (I3A).



**CLAUDIO CARRETERO** (Senior Member, IEEE) received the B.Sc. and M.Sc. degrees in physics, the B.Sc. and M.Sc. degrees in electrical engineering, and the Ph.D. degree in electrical engineering from the University of Zaragoza, Zaragoza, Spain, in 1998, 2002, and 2010, respectively. He is currently an Assistant Professor with the Department of Applied Physics, University of Zaragoza. His research interests include induction heating applications and electromagnetic modeling of inductive systems. He is a member of Instituto de Investigación en Ingeniería de Aragón (I3A).



**SERGIO LLORENTE** received the M.Sc. and Ph.D. degrees in electronic engineering from the University of Zaragoza, Zaragoza, Spain, in 2001 and 2016, respectively. In 2001, he joined Bosch-Siemens Home Appliances Group, Zaragoza, where he held different positions in the Research and Development Department of Induction Cooktops. He has also been an Assistant Professor with the University of Zaragoza, since 2004. He is currently in charge of several research lines and projects and is also an inventor with more than 200 patents. His research interests include power electronics, simulation and control algorithms for power electronics, and temperature.



**JOSÉ M. BURDIO** (Senior Member, IEEE) received the M.Sc. and Ph.D. degrees in electrical engineering from the University of Zaragoza, Zaragoza, Spain, in 1991 and 1995, respectively. In 2000, he was a Visiting Professor with the Center for Power Electronics Systems, Virginia Tech. He has been with the Department of Electronic Engineering and Communications, University of Zaragoza, where he is currently a Professor, the Head of the Group of Power Electronics and Microelectronics, and the Director of the BSH Power Electronics Laboratory, University of Zaragoza. He is the author of more than 80 international journal articles and over 200 papers in conference proceedings and the holder of more than 60 international patents. His main research interests include modeling of switching converters and resonant power conversion for induction heating and biomedical applications. He is a Senior Member of the IEEE Power Electronics Society and the IEEE Industrial Electronics Society. He is also a member of Instituto de Investigación en Ingeniería de Aragón (I3A).

• • •